Archaeometric characterization of prehistoric pottery from Baħrija, Malta

Davide Tanasi[a,*], Daniele Brunelli[b], Valentina Cannavò[b], Sara Tiziana Levi[c]

[a] Department of History, University of South Florida, Tampa, FL, USA
[b] Dipartimento di Scienze Chimiche e Geologiche, Università di Modena e Reggio Emilia, Modena, Italy
[c] Department of Classical and Oriental Studies, Hunter College, City University of New York, NY, USA

ABSTRACT

The end of prehistory in the Maltese archipelago is characterized by the production of a problematic class of pottery, until now attested just at the site of Baħrija, on the western coast of Malta. Such a production represents a break with the tradition in terms of repertoire of shapes, style and technology and it has been interpreted as the result of contact between locals and foreign immigrants. The recent overall reappraisal of the unpublished ceramic assemblage collected during the excavations carried out at Baħrija, represents a unique opportunity to focus on the technological aspects of the production, trying to shed light on the issue of the break with the tradition and the impact of external influxes. Petrographic analysis on thin sections and chemical analyses via X-ray fluorescence spectroscopy (XRF) and laser ablation-inductively coupled plasma mass spectroscopy (LA-ICP-MS) have been carried out to characterize the Baħrija pottery production in order to interpret from a different angle the issue of the possible arrival of newcomers and establishment of a foreign enclave in Malta, which until now has been hypothesized only on the basis of the sudden emergence of the Baħrija pottery.

1. Introduction

Dating to the Oligo-Miocene era of the Tertiary period, the geology of the Maltese islands is entirely composed of sedimentary rock (Fig. 1). The basic geology, when observable in undisturbed horizontal stratification, is constituted by four distinct rock layers: Upper Coralline Limestone, Blue Clay, Globigerina Limestone and Lower Coralline Limestone (Pedley et al., 2002). Exposed Lower Coralline and Globigerina Limestone deposits mainly cover areas of central and southern Malta. The Upper Coralline Limestone is the youngest rock formation and one of its subdivisions is composed of carbonate mudstones, the Mtarfa Member, and can be easily quarried. The Blue Clay is the considered the most important rock horizon, as it has determined the presence an accessible water table (perched aquifer) which was largely exploited in antiquity (Buhagiar, 2012).

From an archaeological point of view, the prehistory of Malta can be summarized by three main macro cultural phases, each of them internally subdivided in multiple chronological and artistic facets (Malone et al., 2009) The first period (Neolithic), ranging from at least 5000 BCE to ca. 4100 BCE and encompassing the cultures of Għar Dalam, Grey Skorba and Red Skorba, marks the beginning of the population of the Maltese islands and is characterized by a strong connection with the contemporaneous cultures of Sicily due to its geographic proximity (Sagona, 2015). The second period (Temple Period), dated to ca. 4100–2400 BCE, represents the climax of Maltese prehistory with the development of one of the most splendid megalithic civilizations in the Mediterranean region, culminating with the culture of the Tarxien Temple. Although, such a phase appears to correspond to a prolonged time of isolationism, in which the communities of the Maltese Archipelago reached a sort of self-sufficiency which translated into the interruption of external relations, above all with Sicily (Bonanno, 2008). The third macro cultural phase (Bronze Age) (Fig. 2), from ca. 2400 to 700 BCE, is characterized on one side by the resumption of its relationship with Sicily with strong evidence of Maltese presence there, and by the arrival of groups of immigrants in the Archipelago which would contribute to the development of the Tarxien Cemetery culture, representing the Early Bronze Age. The appearance of the first Mycenaean goods together with cultural elements derived by Sicilian cultures marks the subsequent Borġ in-Nadur period (Middle Bronze Age), which represents the last Maltese prehistoric culture before Phoenician colonization in the course of the second half of the 8th century BCEE (Tanasi and Vella, 2014).

The terminal part of this last period, essentially being the end of prehistory in the Maltese archipelago, still represents the most problematic phase for archaeological research in the country. In the traditional sequence of Maltese prehistory, there is no placeholder for the
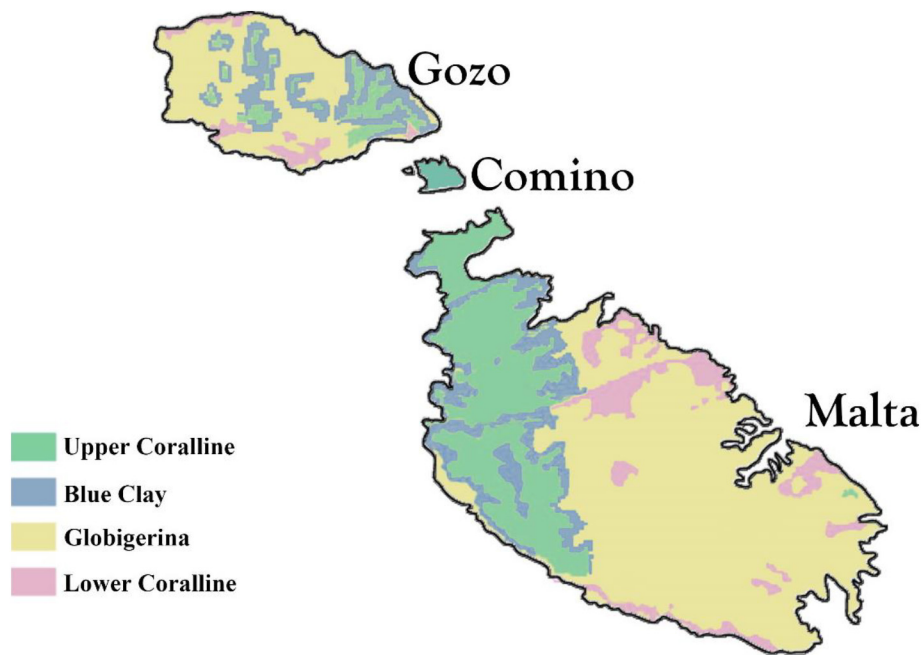

Fig. 1. Geological map of the Maltese islands.
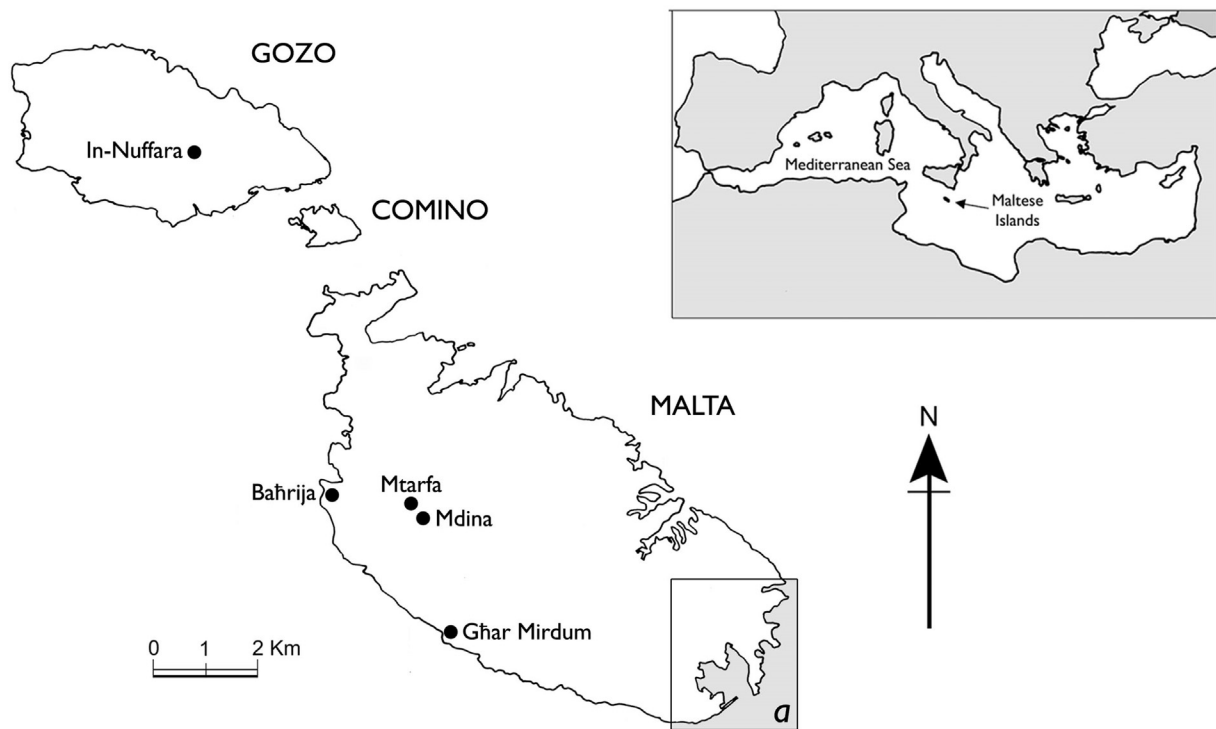(After Pirone and Tykot, 2017).

Fig. 2. Principal Early and Late Bronze Age sites on the Maltese Islands.
(Recchia and Fiorentino, 2015).

Iron Age. There is instead an eight-century long Middle/Late Bronze Age (ca. 1500–700 BCE) represented by the Borġ in-Nadur culture which in part de facto summarizes the Maltese Iron Age. The Phoenician colonization of the island marked the end of prehistory in Malta, though its exact chronology is at the center of an open debate (Vella, 2005; Sagona, 2008, 2011). Certainly the arrival of a foreign culture did not put an end to the local production and the traditional culture kept on fading slowly and gradually into Phoenician by around 700 BCE.

In the absence of substantial cultural changes a progressive series of five pottery styles provides an internal chronological structure for this culture, though they are not yet supported by absolute dates, consisting of Early, Classic and Late Borġ in-Nadur (EBN, CBN, LBN), Painted Ware, and Baħrija (Tanasi, 2015a, 2018). Painted Ware and Baħrija are traditionally considered to be the last expression of the local culture, chronologically parallel with the Sicilian Iron Age. For the repertoire of shapes, technology, and decoration techniques, Baħrija pottery represents a break with tradition (Trump, 1961) and its introduction in

the archipelago has been traditionally explained with a migratory phenomenon of new groups moving from southern Italy towards western Sicily first and ultimately towards Malta (Evans, 1953), on the basis of formal and stylistic analogies between the Baħrija pottery with the Proto-Elymian pottery from Sicily (Tusa, 1992; Vella et al., 2011, 267).

Such Baħrija pottery has practically only been found in the eponymous settlement of Baħrija, on the eastern coast of Malta, associated with other cultural features typical of the Late Borġ in-Nadur *facies*. Such evidence seems to suggest that it cannot be considered as the indicator of a new *facies* but that it is instead just a pottery style characterizing the last phase of Borġ in-Nadur culture in a specific site, which was probably directly affected by the arrival of newcomers (Bonanno, 2017).

The recent overall reappraisal of the unpublished ceramic assemblage collected during the previous excavations carried out at Baħrija (Tanasi, in press) represents a unique opportunity to focus on the technological aspects of the production, trying to shed light on the issue of the break with the tradition and the impact of external influxes. An archaeometric study of the Baħrija pottery helps to finally understand the role of the class of materials with respect to the previous Borġ in-Nadur pottery production and to eventually revise the interpretation of the site of Baħrija as a venue for an enclave of foreigners.

2. Materials

The materials selected for the present study include the main classes of the pottery attested at the site of Baħrija from the excavations carried out by Peet (1910) and Trump (1961). The direct examination of a large unpublished group of materials was carried out in the summer of 2017 and led to the definition of several classes of pottery based on the features of their fabric: three types of fine table ware [*orange ware*, *grey ware,* and 'traditional' *Baħrija ware*, the only one known in the literature (Evans, 1971)]; three of semi-fine/coarse ware (*orange-grey unslipped ware*, *dark yellow coarse ware* and *red slipped coarse ware*), and one class of cooking ware. The orange-grey unslipped fabric has same features of Tanasi fabric 3 identified at the Borġ in-Nadur settlement (Tanasi, 2015a tab. 3, p. 39; Barone et al., 2015, p. 101, tab. 2). In the assemblage from Baħrija, the Borġ in-Nadur reddish yellow fabric with dark red-to-black mottled slip (Tanasi fabric 4: Barone et al., 2015, p. 100, tab. 1) as well as the Borġ in-Nadur painted/dribbled ware (Barone et al., 2015, p. 101, tab. 2), both chronologically attributed to Trump's phase II B3 (Tanasi, 2015a, tab. 3, p. 39) were also both well attested.

The orange ware has a medium/hard fabric, with lithic inclusions (very fine 10%) and voids (very fine-fine 2%), dark orange/light brown surfaces (from 7.5YR 6/6 to 10YR 6/8), and a blackish core; sometimes its shows a red slip or in its absence surfaces are always burnished.

The *grey ware* shows a very hard fabric, with no detectable inclusions and voids (very fine-fine 2%), grey surfaces with blackish core; it is unslipped, but surfaces are always burnished. A class of cups belonging to this category has a plastic decoration or dark red burnished slip. Due to the presence of dark grits in the fabric and a peculiar typology, this class has also been cautiously interpreted as being possible imports from Middle Bronze Age Sicily (Vella et al., 2011).

The 'traditional' *Baħrija ware* has a very fine hard fabric with very few voids and inclusions (15%); surfaces are slipped in very dark brown (10YR 3/2) or black color. It occurs mostly on bowls and dippers cups with the peculiar excised labyrinthine patterns filled with white paste.

The *orange-grey unslipped fabric* shows a very hard fabric, with lithic inclusions (very fine 10%) and voids (very fine-fine 2%) with orange-grey surface (from 5 YR 7/6 reddish yellow to 7.5 YR 7/3 pink), and a dark grey core (5 Y 4/1 dark grey); it is unslipped and generally undecorated.

The dark yellow coarse ware has a medium fabric, with lithic inclusions and grog (fine 15%) and voids (fine 15%), dark orange surfaces (7.5YR 6/6), and a dark grey core; it is always unslipped and sometimes

it has plastic linear decoration.

The *red slipped coarse ware* displays a very hard fabric with lithic and dark inclusions (very fine-fine 2%), darker core, very sandy surfaces, and very thin red slip.

Following the same protocol used with the pottery from Borġ in-Nadur *facies* found at the eponymous temple (Tanasi, 2011a; Raneri et al., 2015), in order to characterize the pottery production documented at Baħrija and to provide new data to the open debate on the existence of a Baħrija *facies*, a selection of samples representing all the classes was subjected to petrographic and chemical analyses.

In particular, four examples of grey ware showing typical features of Sicilian Middle Bronze pottery production (100061B, 100050A, 100061E, 100061H), two examples of strainer spouted jars in painted ware (100051D, 100109A) and a wall fragment of painted ware (100109B), all traditionally considered as Sicilian imports (Vella et al., 2011), were analysed in order to clearly establish their origin. Finally, a sample of a pyramidal loom weight (100006A) with a very peculiar fabric was analysed as its fabric appeared to be rather different and peculiar already during the macroscopic examination.

3. Methods

Thirty-seven samples (26 potsherds and 1 loom weight) representing different ware types identifiable in the Baħrija ceramic assemblage were selected for archaeometric investigation, petrography and chemical analysis (Table 1). Analyses were carried out at the University of Modena and Reggio Emilia (Italy) in the Department of Chemical and Geological Sciences and at the Centro Interdipartimentale Grandi Strumenti (CIGS).

Petrographic thin sections were described with a polarizing microscope following the standard proposed by Whitbread (1989) and by Quinn (2013). Major elements bulk composition of 37 samples was assessed by X-ray fluorescence spectroscopy (XRF). Minor and trace elements were measured by XRF and laser ablation-inductively coupled plasma mass spectroscopy (LA-ICP-MS). The latter technique was adopted 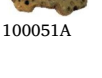to ensure the analyses of six samples for which only the small volume of material was available (< 300 mg), not allowing the measurement by XRF of minor and trace elements.

XRF analysis was carried out with a Philips PW 1480 instrument preparing boric acid tablets with 300 or 150 mg of calcinated powder. External standard calibration was based on GBW 07701–07711 international standards (Chunshu et al., 1996) following the procedure defined in Gazzulla Barreda et al. (2016). Detection limits for the analysed elements are as follows: Cu 50 ppm; Zn 20 ppm; As 10 ppm; Pb 20 ppm; V 10 ppm; Cr 10 ppm; Co 10 ppm; Ni 10 ppm; Ba 25 ppm; Ce 20 ppm; Nb 2 ppm; Zr 50 ppm; Sr 20 ppm; Y 20 ppm; La 25 ppm; Rb 40 ppm; Sb 20 ppm.

LA-ICP-MS analyses were obtained by a Nd:YAG deep UV (213 nm) New Wave Research UP-213 laser ablation system (LA) coupled to a Thermo Fisher Scientific X-Series II induced coupled plasma mass spectrometer (ICP-MS). Instrumental drift correction was computed following the procedure reported in Brunelli et al. (2013) using glass beads of NIST 610, NIST 612 and NIST 614 as external standards and ^{29}Si as an internal standard. Data reduction was performed with Plasma Lab® software by Thermo Scientific. The most crucial stage in multi-element analysis by LA-ICP-MS of silicate matrices like the ancient pottery is the sample preparation. We adopted the fusion technique procedure, which is one of the best suited for plasma atomization (Papadopoulou et al., 2004). Glass pearls were prepared by melting at 1300 °C for 1 h a quota of 50 mg of the sample mixed with a ten-fold amount (500 mg) of lithium metaborate puratronic in a Pt-Au-Rh crucible. This procedure induces the evaporation of some volatile elements such as Rb. Its value cannot be quantified accurately and is therefore omitted in the final measures (Condie, 2015). Resulting concentrations must be corrected for the pollution introduced by the crucibles and the melting agent. The use of lithium metaborate and Pt-Au-Rh crucibles

Table 1

List of samples from Baħrija with indication of shape and pottery class grouped according to ware types.

Obj. photo and ID. no.	Shape	Class	Obj. photo and ID. no.	Shape	Class
100041N	Cup	Orange ware	100034A	Dipper cup	Orange ware
100034K	Cup	Orange ware	100042D	Cup	Orange ware
100050B	Juglet	Orange ware	100041H	Cup	Grey ware
100041M	Cup	Grey ware	100041D	Cup	Grey ware
100050A	Juglet	Grey ware *Sicilian import?*	100061B	Cup *Sicilian import?*	Grey ware (foreign?)
100061E	Cup *Sicilian import?*	Grey ware (foreign?)	100061H	Cup *Sicilian import?*	Grey ware (foreign?)
100061A	Cup	Grey ware (foreign?)	100067	Bowl	Traditional *Baħrija* ware
100031C	Dipper cup	Traditional *Baħrija* ware	100033G	Dipper cup	Traditional *Baħrija* ware
100094A	Bowl	Traditional *Baħrija* ware	100033C	Dipper cup	Traditional *Baħrija* ware
100040C	Cup	Borġ in-Nadur reddish yellow fabric with dark red/black mottled slip	100031G	Dipper cup	Borġ in-Nadur reddish yellow fabric with dark red/black mottled slip
100039A	Jar	Borġ in-Nadur reddish yellow fabric with dark red/black mottled slip	100051D	Strainer wall *Sicilian import?*	Painted/Dribbled ware
100109A	Strainer wall *Sicilian import?*	Painted/dribbled ware	100109B	Wall *Sicilian import?*	Painted/dribbled ware
100085A	Jar	Orange-grey unslipped ware	100087C	*Pithos*	Orange-grey unslipped ware
100083B	Lid	Orange-grey unslipped ware	100051B	Strainer	Orange-grey unslipped ware
100051C	Strainer	Orange-grey unslipped ware	100051A	Strainer	Orange-grey unslipped ware

Table 1 (*continued*)

Obj. photo and ID. no.	Shape	Class	Obj. photo and ID. no.	Shape	Class
100088B	*Pithos*	Red slipped coarse ware	100087D	*Pithos*	Red slipped coarse ware
100088A	*Pithos*	Red slipped coarse ware	100088C	*Pithos*	Dark yellow coarse ware
100088D	*Pithos*	Dark yellow coarse ware	100084A	Jar	Cooking ware
100006A	Loom weight *Foreign import?*	–			

hinders the definition of related elements including Li, K, B, Rh, Cs, Re, Os, Pt, Au and Hg. The correction is done by subtraction of the blank composition obtained in the crucible without the sample and measured in the same analytical conditions by LA-ICP-MS together with the unknown samples. All plotted values are normalized on the average composition of the upper continental crust (Rudnick and Gao, 2003).

Principal components analysis (PCA) was performed using the SPSS 17.0 statistical package on chemical data. This approach helps the definition of the compositional groups and for the chemical comparison data of pottery and sediments.

4. Results

4.1. Petrography

The analysis of the thin sections allowed characterizing and classifying the samples into three fabrics based on the different nature of the temper added to the clays during the preparation of the paste ware. Two are characterized by temper's clasts pertaining to sedimentary rock fragments, and one whose clasts show a temper deriving from intrusive magmatic (granitic) rock fragments (Table 2 and Fig. 3).

The classificatory system here adopted is organized in Groups, linked to the geological/lithological nature of the tempers (I = Intrusive, S = Sedimentary), and Fabrics (labelled by numbers) according to a general criteria proposed for Central Mediterranean prehistoric pottery (Levi et al., 2017).

Accordingly, we defined Fabrics S1 and S2 as characterized by the presence of calcareous clay, rich in microfossils and common micrite

deriving from sedimentary rocks compatible with the geological units present in the Maltese terrain, such as Upper Coralline Limestone, Lower Coralline Limestone and Globigerina Limestone (Oil Exploration Directorate, 1993). A markedly different Fabric I1 is defined for pottery temper rich in rock fragments deriving from granitic intrusions. This kind of lithology is not present in the local (on island) geology and sedimentary record.

S1. Fossiliferous, optically inactive groundmass
Coarse:fine:voids (c:f:v) 10:85:5 to 10:85:7

This fabric is characterized by a fine optically inactive calcareous groundmass, rich in foraminifera; the coarse fraction is weakly attested and is composed by only grog temper.

The voids are few to common; *meso* channels and vughs are also commonly attested and few macro vughs and planar channels, and very rare mega vughs characterize the microstructure. The voids sometimes have a long axis orientation parallel with the vessel margins and they are single-spaced. Some of the voids are infilled or partially infilled with secondary calcite.

The groundmass is generally homogeneous throughout the sections; the color is dark brown in PPL and XPL. The micromass is optically slightly inactive, suggesting a fairly high firing temperature. Samples 100034A and 100041N have a reddish slip on their external margins and sample 100034K is characterized by a double structure: one dark brown in PPL and XPL, the second dark red in PPL and XPL.

The inclusions appear to have a unimodal size distribution: they are moderately sorted with a random orientation and they are open-spaced.

Table 2
Composition of Baħrija pottery fabrics.

Fabric	Dominant 50-70%	Frequent 30-50%	Common 15-30%	Few 5-15%	Very few 2-5%	Rare 0,5-2%	Very rare <0,5%
S1. Fossiliferous optically inactive groundmass	Microfossils		Grog	Calcimudstone (micrite)			
S2a. Grog in homogeneous fossiliferous groundmass	Microfossils	Grog		Calcimudstone (micrite)	Vegetable fiber	Opaque minerals	Spatic calcite, Monocrystalline quartz
S2b. Grog in inhomogeneous fossiliferous groundmass	Microfossils	Grog		Calcimudstone (micrite)		Monocrystalline quartz	
I1. Granite	Granite	Quartz			Iron oxides		

Fig. 3. Petrographic classification of the fabrics, photographed through polarizing microscope (PPL and XPL) (width image 5.5 mm). S1 Fossiliferous optically inactive groundmass; S2a Grog in homogeneous fossiliferous groundmass; S2b Grog in inhomogeneous fossiliferous groundmass; I1 Granite.

The coarse fraction (1.2 to 0.2 mm) is commonly composed by grog, generally with subangular equant and elongated clasts (< 1.2 mm).

Two types of grog were identified: dark brown-black opaque, optically inactive, with no minerals visible inside; and fossiliferous dark brown and black clasts, optically inactive, characterized by the presence of microfossils, mainly foraminifera.

Micrite, with equant, subrounded clasts (< 0.45 mm) and foraminifer fossils are weakly attested, while the fine fraction (< 0.2 mm) is dominated by microfossils, mainly foraminifers and the micrite is also commonly attested. Sample 100034K differs for the very few amounts of microfossils, while the other properties of the groundmass are compatible with the general characters of the fabric.

S2. Grog, fossiliferous groundmass

This fabric is characterized by a coarse fraction, composed mainly by grog, and a fossiliferous groundmass; it is divided in two variants on the base of matrix characteristics.

S2a. Grog in homogeneous fossiliferous groundmass
c:f:v 10:85:5 to 15:78:7

This variant is characterized by homogeneous calcareous clay, rich in foraminifera. The optical activity of the groundmass suggests a fairly low firing temperature.

In the microstructure are present common voids, frequent *meso* channels and vughs; also common macro vughs and planar channels, and common to few mega vughs are identifiable. The voids have mainly a long axis orientation parallel with the vessel margins and they are single-spaced to closed-spaced, most of them infilled with secondary calcite.

The groundmass is generally homogeneous and well compacted throughout the sections, although some samples (10087C, 100085A, 100050A, 100051C, 100041M, 100051B) show variability in the micromass, specifically color variations, sometimes associated with different crystallitic concentrations.

The color varies from yellowish and reddish brown to brown in PPL, and light brown to dark brown in XPL. The sample 100050B shows a sandwich structure with a wide reducing phase between two slim oxidising phases. Some samples show the presence of slip marks on the surfaces. The micromass is optically active and sometimes the secondary calcite is spread through it.

The inclusions have a bimodal size distribution and are moderately sorted, with a random orientation and open-spaced.

The coarse fraction (1.5 to 0.3 mm) is characterized by the frequent presence of grog, with generally subangular equant and elongated clasts (< 1.5 mm). Two types of grog are clearly identified, as attested in the previous fabric, and in two samples (100085A and 100087C) the grog clasts have a maximum length of 3 mm.

Few micrite, with equant, subrounded clasts (< 0.45 mm) and foraminifer fossils are also present.

In samples 100031C, 100061H, and 100084A the micrite has a max length of ca. 1.2 mm, with microfossils and occasionally monocrystalline quartz. Very few burnt vegetable fibers (< 5.1 mm) and rare opaque minerals are visible in thin sections, and very rare spathic calcite, with angular equant clasts, is present only in sample 100088B.

Foraminifer microfossils dominate the fine fraction (< 0.3 mm) and micrite is also frequently attested. Commonly grog temper is also present and finally monocrystalline quartz is rarely attested.

S2b. Grog in inhomogeneous fossiliferous groundmass
C:f:v 10:85:5 to 15:78:7

This variant is characterized by an inhomogeneous calcareous, not well-packed groundmass.

The microstructures are few to common voids and frequent *meso* channels and vughs. Also, common macro vughs and planar channels, common to few mega vughs are attested. The voids have mainly a long axis orientation parallel with the vessel margins and they are single-spaced to closed-spaced. Most of the voids are free from secondary calcite.

The groundmass is generally heterogeneous throughout the sections; the micromass evidences irregular distribution and seems to show that the ceramic paste would hardly melt during the preparation.

The micromass is optically active and the color varies from yellowish and reddish brown to brown in PPL, and light brown to dark brown in XPL. Samples 100042D and 100088B show a sandwich structure with a reducing phase between two oxidising phases.

The inclusions have a bimodal size distribution; they are moderately to poorly sorted. They have random orientation and they are open-spaced.

The coarse fraction (3 to 0.3 mm) is characterized by the frequent presence of grog, generally with subangular equant and elongated clasts (< 1.5 mm); two types of grog, as described in the previous fabric, are always present.

Foraminifera microfossils are commonly attested, and some species can be identified: globigerina, echinoderm spines, gastropods, and Discocyclina (< 1.8 mm). Some of the microfossils have the body infilled by iron oxides. Finally, few micrite, with equant and subrounded clasts, are spread in the matrix (< 0.9 mm).

Foraminifer fossils (mainly globigerina) dominate the fine fraction (< 0.3 mm) and then micrite, grog and monocrystalline quartz are attested with decreasing percentages.

I1. Granite
c:f:v 25:68:7

Coarse and angular fragments of granitic rocks and quartz minerals, set in a glassy reddish groundmass, characterize this fabric, attested only in one sample, thus suggesting that the clay base is essentially high-fired.

The microstructures are mainly composed by voids; these comprise few *meso* vughs and common macro and mega vughs. The voids are not infilled with calcitic material, they have a random orientation and they are single-spaced.

The groundmass is homogeneous throughout the section; the color is dark red in PPL and very dark red in XPL. The micromass is totally optically inactive and has a "glassy" texture.

The inclusions have a bimodal grain-size distribution and are poorly sorted. They have a random orientation and they are closed-spaced.

The coarse fraction (4.2 to 0.3 mm) is dominated by granite rocks fragment, with equant and elongated, angular clasts; the most attested mineral is quartz, with equant and elongated, angular clasts (< 3 mm). Finally, there are very few iron oxides, with equant subrounded clasts < 0.35 mm.

The fine fraction (< 0.3 mm) is mainly composed by quartz with equant and elongated, angular clasts and by iron oxides, with equant subrounded clasts.

4.2. Chemistry: XRF and LA-ICP-MS

Fabric classification based on petrography has been compared with the chemical composition, based on major and minor element variability (Tables 3, 4). Average and standard deviation of the local fabrics are reported in the table below (Table 5). To validate the data performed by XRF and LA-ICP-MS, we compare the concentrations of element analysed by both techniques. The plot (Fig. 4) shows the TiO_2 wt% determined by XRF correlated with a high linearity with TiO_2 wt% determined by LA-ICP-MS measurements ($R^2 = 0.8987$).

According to the major elements, Fabric S1 is characterized by a higher content of SiO_2, MgO, Al_2O_3, and Fe_2O_3, and lower CaO content. Minor and trace elements reveal weak differences between Fabrics S1 and S2 that can be explained in the reduced compositional range of local raw materials. The Granite Fabric is slightly distinguishable for the SiO_2 content, which is extremely high in comparison with the other samples; by contrast the MgO, CaO and Fe_2O_3 contents are the lowest of the whole dataset. Concerning the minor and trace elements, the Fabric appears extremely depleted with most elements below the detection

Table 3
Major elements (wt%) of Baħrija pottery measured by XRF fluorescence.

Fabric	sample	shape	SiO2	MgO	Al2O3	Na2O	P2O5	K2O	CaO	TiO2	MnO	Fe2O3	LOI
S1. Fossiliferous optically inactive groundmass	100034A	dipper cup	43,79	3,45	17,78	0,52	0,27	1,57	13,06	0,89	0,04	7,49	11,17
	100034K	cup	46,43	3,10	17,43	0,67	0,38	1,97	12,10	0,88	0,05	9,21	7,78
	100040C	cup	47,83	3,22	18,95	0,76	0,32	2,32	14,64	0,93	0,05	8,38	2,61
	100041H	cup	46,28	3,35	18,55	0,69	0,48	1,93	12,43	0,87	0,05	7,25	8,11
	100041N	cup	45,71	3,07	18,13	0,76	0,42	2,01	13,21	0,88	0,05	7,43	8,33
	100061B	cup	47,02	3,22	18,25	0,81	0,38	2,13	13,12	0,90	0,05	7,62	6,51
S2a. Grog in homogeneous fossiliferous groundmass	100031C	dipper cup	42,00	2,60	15,39	0,64	0,29	1,53	15,15	0,75	0,03	6,37	15,25
	100031G	dipper cup	43,92	2,81	16,35	0,65	0,45	1,45	12,02	0,78	0,04	7,20	14,34
	100039A	jar	46,58	3,03	19,00	0,73	0,30	1,91	12,20	0,86	0,04	7,77	7,59
	100041M	cup	42,09	2,63	15,95	0,71	0,20	1,59	15,39	0,80	0,04	6,94	13,66
	100050A	juglet	39,80	2,60	14,35	0,48	0,24	1,38	15,79	0,75	0,04	5,95	18,61
	100050B	juglet	44,45	2,70	16,64	0,57	0,32	1,65	15,92	0,92	0,05	7,42	9,39
	100051D	strainer	39,80	2,59	14,37	0,65	0,42	1,46	19,70	0,73	0,04	6,58	13,64
	100061E	cup	48,06	2,46	18,03	0,71	0,30	2,07	8,93	0,93	0,04	7,52	10,95
	100061H	cup	44,49	3,04	16,94	0,81	0,33	1,90	15,08	0,81	0,05	7,10	9,47
	100067	bowl	47,00	2,78	18,25	0,81	0,22	2,17	8,81	0,89	0,04	7,41	11,60
	100084A	jar	37,45	2,49	13,68	0,25	0,19	1,22	15,57	0,68	0,05	6,09	22,33
	100085A	jar	37,91	2,32	15,51	0,34	0,17	1,08	13,14	0,80	0,05	6,98	21,71
	100087C	pithos	37,58	2,38	13,67	0,45	0,30	1,30	18,40	0,73	0,05	6,10	19,04
	100088B	pithos	41,38	2,51	15,14	0,57	0,29	1,45	14,88	0,75	0,04	6,16	16,84
	100088D	pithos	35,01	2,38	12,68	0,27	0,33	1,05	18,04	0,67	0,05	5,59	23,93
	100094A	bowl	46,25	2,76	18,48	0,76	0,24	2,29	11,65	0,87	0,04	7,36	9,30
	100109A	strainer wall	43,95	2,61	17,31	0,54	0,35	1,62	15,21	0,86	0,04	6,84	10,68
	100033G	dipper cup	44,96	2,62	18,25	0,52	0,27	1,53	10,70	0,89	0,04	9,10	11,12
	100051B	strainer	41,40	2,47	16,12	0,61	0,26	1,54	14,49	0,79	0,03	6,76	15,53
	100051C	strainer	40,00	2,39	15,14	0,47	0,24	1,43	14,37	0,79	0,03	6,79	18,34
S2b. Grog in inhomogeneous fossiliferous groundmass	100042D	cup	40,43	2,02	17,22	0,57	0,29	1,39	11,61	0,86	0,03	7,16	18,43
	100109B	wall	36,73	2,43	13,71	0,42	0,30	1,32	17,68	0,74	0,04	6,42	20,21
	100033C	dipper cup	41,68	2,52	16,30	0,62	0,47	1,67	16,20	0,80	0,03	6,90	12,81
	100041D	cup	44,60	2,79	16,94	0,71	0,29	1,68	12,71	0,81	0,03	6,59	12,84
	100051A	strainer	39,21	2,42	16,14	0,39	0,51	1,37	16,12	0,87	0,05	7,54	15,38
	100061A	cup	34,95	1,82	13,48	0,32	0,26	1,15	21,06	0,75	0,03	6,54	19,64
	100083B	lid	41,82	2,55	15,73	0,58	0,31	1,61	15,73	0,80	0,03	6,83	14,01
	100087D	pithos	33,31	2,42	12,02	0,29	0,39	0,87	20,97	0,69	0,05	6,16	22,87
	100088A	pithos	41,41	2,89	15,01	0,69	0,24	2,18	13,19	0,75	0,04	6,46	17,13
	100088C	pithos	43,71	2,54	16,64	0,53	0,28	1,45	10,55	0,83	0,04	6,89	16,53
I1. Granite	100006A	loom weight	79,02	0,62	16,18	0,36	0,01	1,35	0,28	0,16	0,06	1,65	0,32

limit and the lowest contents in V, Ba, Zr, Zn, Cu have, on the contrary, a very high Rb content. This concentration should be also affected by enrichment, with Rb one of the most susceptible alkali metals for post-depositional alteration (Hunt, 2017).

The composition of the six samples analysed by LA-ICP-MS (all belonging to Fabric S2) is reported in the table below (Table 6). Element concentrations are plotted in order of incompatibility in Fig. 5a. This order reflects the geochemical behavior of the elements showing their tendency to form the rocks of the continental crust starting from their basic constituent represented by primary magmatism. Two subsets of elements, the Rare Earth Elements (REE) and transition metals (Ti, V, Cr, Mn, Co, Ni, Cu, Zn), are plotted in Fig. 5b and c respectively. Less important negative anomalies are represented by a light depletion in Ba, followed by another in Zr and Hf (Fig. 5a).

Looking to the REE subset (Fig. 5b), it is noticeable that light REE (LREE from La to Sm) tend to be more enriched than heavy ones (HREE: from Dy to Lu). A sinusoidal trend that enriches selectively adjacent elements is, however, clear.

The transition metals (Fig. 5c) present a complex pattern with prominent Mn, Co, and Ni depletion and Cu enrichment with respect to the almost non-fractionated Ti and V contents. The scatter of the measured samples increases however from left to right in the chosen element order.

5. Discussion

Compositional analyses of our samples allowed the identification of

two local fabrics, S1 and S2, and an imported specimen.

Considering the relationship between shape/function and fabrics in the present dataset the finer Fabric S1 is only used for cups while the grog fabric was used for all the shapes with a prevalence of the in-homogeneous S2b for the larger, and possibly coarser, *pithoi* (Fig. 6).

The grey wares (100061B, 100050A, 100061E, 100061H) that show typical features of Sicilian Middle Bronze pottery production are all characterized by S2a fabric, except for 100061B (S1). The two examples of strainer spouted jars in painted ware (100051D, 100109A) are both classified as S2a fabric and the undecorated one (100109B) is the only defined in S2b fabric. Overall the shapes traditionally considered as Sicilian imports (Vella et al. 2010) are locally produced and the only imported sample is a loom weight.

This result is coherent with other studies of Bronze Age pottery from Malta (Barone et al., 2015; Jones et al., 2014) outlining the scarcity of imported vessels compared with other insular environments in the Mediterranean, for example the Aeolian Islands (Williams, 1980, 1991; Levi and Jones, 2005; Levi and Fragnoli, 2010; Jones et al., 2014; Levi et al., 2019).

In general, Bronze Age pottery from Malta shows a relative homogeneity in its local production with the use of fossiliferous clay tempered with grog and/or calcite. Despite that, the groundmass is sometimes inhomogeneous, suggesting clay mixing during the paste preparation. The correspondences between the present study and others (Barone et al., 2015; Jones et al., 2014) are proposed in the table below (Table 7). In particular, Fabric S2 is coherent with Borġ in-Nadur Barone's Fabric A (coarse grog and fine quartz inclusions, groundmass with

Table 4

Minor and trace elements (ppm) of Baħrija pottery measured by XRF fluorescence and LA-ICP-MS (with asterisk).

Fabric	sample	shape	V	Cr	Co	Ni	Cu	Zn	Rb	Sr	Y	Zr	Ba	La	Ce	Nd
S1. Fossiliferous optically inactive groundmass	100034A	dipper cup	219	234	23	87	93	180	95	693	34	262	348	79	157	37
	100034K	cup	201	183	26	65	192	162	119	590	30	220	1025	45	109	29
	100040C	cup	270	186	11	62	90	142	111	683	28	245	274	42	149	31
	100041H	cup	189	169	16	43	99	129	97	614	23	203	253	46	89	31
	100041N	cup	206	201	11	61	91	149	105	641	30	225	404	52	113	33
	100061B	cup	170	165	13	44	107	115	87	589	18	182	306	46	68	33
S2a. Grog in homogeneous fossiliferous groundmass	100031C	dipper cup	132	151	15	55	111	124	95	745	25	246	388	38	86	30
	100031G	dipper cup	167	185	14	62	89	149	100	717	21	184	391	51	78	35
	100039A	jar	197	179	14	56	66	165	129	560	35	225	281	45	132	33
	100041M	cup	162	206	10	65	130	156	82	672	22	188	390	50	97	34
	100050A	juglet	155	178	16	58	98	161	105	981	30	242	347	51	124	28
	100050B	juglet	180	199	17	65	104	144	86	715	34	269	339	49	132	34
	100051D	strainer	132	190	17	56	145	126	76	747	24	222	329	54	132	33
	100061E	cup	217	187	13	55	102	137	121	509	35	259	374	53	113	32
	100061H	cup	185	173	15	56	98	164	125	711	31	240	348	54	95	30
	100067*	bowl	122	209	55	234	290	148	0	354	28	175	362	59	90	43
	100084A	jar	128	159	19	49	130	92	65	402	udl	171	362	40	126	28
	100085A	jar	121	124	20	45	111	104	89	370	22	210	329	43	118	30
	100087C	pithos	180	202	18	70	120	151	112	771	29	228	332	60	145	41
	100088B	pithos	151	182	13	55	110	140	107	871	27	223	358	61	109	28
	100088D	pithos	136	170	13	57	114	145	88	818	28	221	428	48	96	25
	100094A	bowl	193	145	16	48	93	130	99	467	20	166	311	46	121	28
	100109A	strainer wall	183	182	20	54	109	158	91	639	32	221	321	43	119	36
	100033G*	dipper cup	128	147	14	68	52	108	8	359G	27	183	243	60	88	41
	100051B*	strainer	108	123	12	50	89	96	8	419	28	187	270	53	83	40
	100051C*	strainer	100	274	12	91	204	179	0	417C	26	193	311	57	75	36
S2b. Grog in inhomogeneous fossiliferous groundmass	100042D*	cup	115	133	11	44	92	78	5	354	26	177	311	56	86	40
	100109B*	wall	93	113	15	51	214	266	0	367	24	162	274	48	70	34
	100033C	dipper cup	158	201	19	69	166	180	103	717	25	245	356	50	134	30
	100041D	cup	152	164	16	47	108	135	99	640	21	171	283	63	102	37
	100051A	strainer	162	201	14	67	117	157	83	715	34	270	414	56	123	34
	100061A	cup	130	145	10	38	159	108	70	597	21	205	368	50	114	34
	100083B	lid	142	161	udl	49	94	109	78	744	27	202	310	50	86	30
	100087D	pithos	137	175	12	67	135	135	71	1012	23	219	381	51	155	29
	100088A	pithos	174	169	15	55	75	117	104	574	29	232	318	48	118	32
	100088C	pithos	177	197	17	64	76	162	105	595	32	265	385	55	140	33
I1. Granite	100006A	loom weight	19	udl	udl	udl	16	45	359	udl	udl	59	36	udl	udl	21

abundant fossil, high-medium birefringence) and with some samples belonging to the same ware found at Ognina and Cannatello (Sicily) but produced in Malta.

Fabric S3 "grog and spathic calcite" is not attested in the present study but has been identified by Barone (Fabric B: abundant grog, spathic calcite, fine quartz inclusions, and fossiliferous groundmass with high birefringence) in another prehistoric data set from Tas-Silġ under investigation by our team (courtesy of Alberto Cazzella and Giulia Recchia). Local production with fossiliferous Blue Clays has been also suggested for Roman amphorae (Bruno and Capelli, 2000).

Other considerations arise by comparing the chemical data of pottery and local clays, in particular Blue Clay from Gnejna Bay (Barone et al., 2015). The vessel distribution shows a linear trend in the SiO_2/CaO vs. Al_2O_3/CaO diagram (Fig. 7a) and a parabolic trend in the SiO_2/MgO vs. Al_2O_3/CaO diagram (Fig. 7b). These relationships suggest variable addition of clay sediments used as raw materials in terms of relative proportion of clay and silt/sand fractions. In fact, the Fabric's groups are distributed along the trends, with the clay specimens falling at their tip.

Plotting also the Fabrics from the Borġ in-Nadur settlement (Barone et al., 2015), the compositional field of samples from Baħrija and Borġ in-Nadur shows two parallel linear trends in the SiO_2/CaO vs. Al_2O_3/CaO diagram (Fig. 8a), with the clay specimens falling at their tip. In the SiO_2/MgO vs. Al_2O_3/CaO diagram (Fig. 8b), the Baħrija Fabrics

distribution differs from the Borġ in-Nadur one, suggesting a depletion in CaO and an enrichment in MgO of the Baħrija samples. This distribution should be explained with the presence of Fabric S3 (Grog and spathic calcite) in the Borġ in-Nadur dataset and with the use of different local raw materials.

Mixing of different clays is attested by the compositional (trends) and petrographic properties of the groundmass. These observations may suggest an attempt of remediating the scarce properties of the raw materials by adding correctional components during the mixing of the paste.

Principal components analysis (Fig. 9), based on major and minor elements, grouped the Fabrics of Baħrija and Borġ in-Nadur sites (Barone et al., 2015). Also the Borġ in-Nadur type pottery recovered from Middle Bronze Age archaeological contexts in Ognina (SR) and in Cannatello (SG) (Raneri et al., 2015) was included because they are considered imports from Malta.

The PCA plot shows some compositional differences between Baħrija and Borġ in-Nadur Fabrics (A and B) compatible with the variability of local raw materials and with use of different temper (spathic calcite) in the case of Fabric B (S3). The overlapping of Maltese imported vessels recovered at Ognina and Cannatello with the local Fabrics from Baħrija and Borġ in-Nadur confirmed their provenance from Malta.

The combined petrographic and chemical analysis of the Baħrija

Table 5
Mean and standard deviation of major, minor and trace elements of the Baħrija fabric groups.

Fabric		SiO2	MgO	Al2O3	Na2O	P2O5	K2O	CaO	TiO2	MnO	Fe2O3
I1. Granite		79,0	0,6	16,2	0,4	0,0	1,3	0,3	0,2	0,1	1,7
S1. Fossiliferous optically inactive groundmass	mean	46,2	3,2	18,2	0,7	0,4	2,0	13,1	0,9	0,0	7,9
	st.dev	1,4	0,1	0,5	0,1	0,1	0,2	0,9	0,0	0,0	0,8
S2a. Grog in homogeneous fossiliferous groundmass	mean	42,2	2,6	16,1	0,6	0,3	1,6	14,3	0,8	0,0	6,9
	st.dev	3,6	0,2	1,8	0,2	0,1	0,3	2,9	0,1	0,0	0,8
S2b. Grog in inhomogeneous fossiliferous groundmass	mean	39,8	2,4	15,3	0,5	0,3	1,5	15,6	0,8	0,0	6,7
	st.dev	3,7	0,3	1,7	0,1	0,1	0,4	3,6	0,1	0,0	0,4

| Fabric		V	Cr	Co	Ni	Cu	Zn	Rb	Sr	Y	Zr	Ba	La	Ce	Nd
I1. Granite		19	udl	udl	udl	16	45	359	udl	udl	59	36	udl	udl	21
S1. Fossiliferous optically inactive groundmass	mean	209	190	17	60	112	146	102	635	27	223	435	52	114	32
	st.dev	31	23	6	15	36	21	11	41	5	26	268	13	31	2
S2a. Grog in homogeneous fossiliferous groundmass	mean	154	178	17	68	118	139	79	612	28	213	341	51	108	33
	st.dev	32	33	9	40	49	24	41	185	4	30	44	7	20	5
S2b. Grog in inhomogeneous fossiliferous groundmass	mean	144	166	14	55	124	145	72	632	26	215	340	53	113	33
	st.dev	25	28	3	10	43	49	37	180	4	36	45	4	26	3
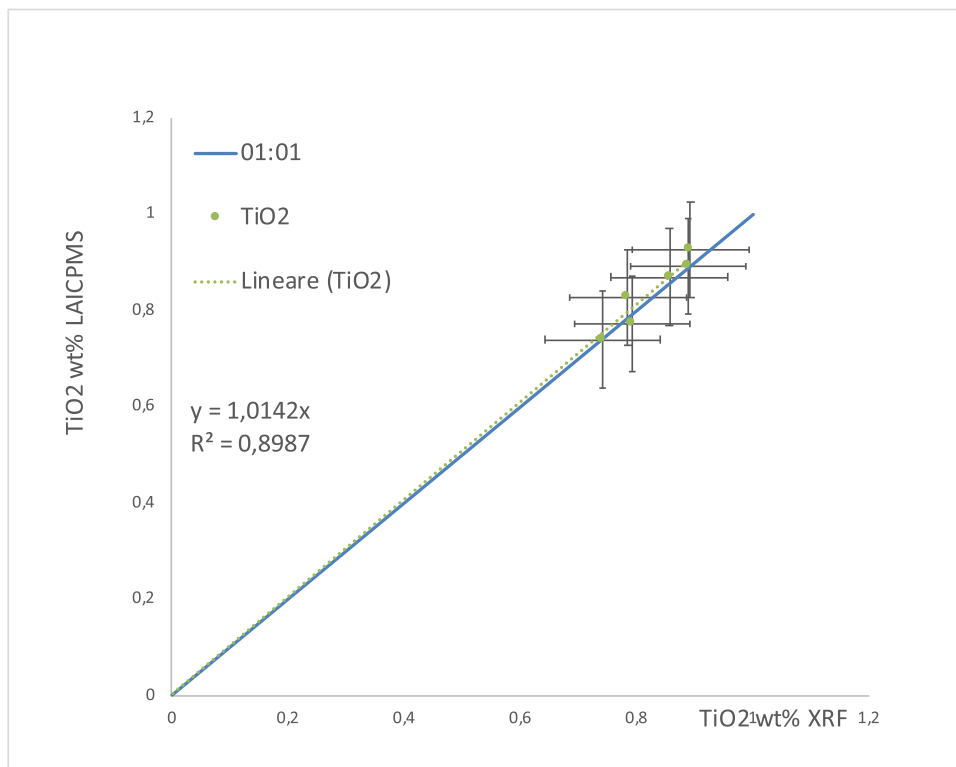
Fig. 4. Comparison between TiO$_2$ wt% measured in Baħrija pottery by XRF and LA-ICP-MS.

Table 6
Major, minor and trace elements (ppm) of the samples measured by LA-ICP-MS (100033G, 100051B, 100051C, 100,067, 100042D, 100109B).

sample	Fabric	P	Ti	V	Cr	Mn	Co	Ni	Cu	Zn	Sr	Y	Zr	Nb	Ba	La	Ce
100033G		1125,7	5348,2	128,1	146,5	193,6	13,9	68,4	52,3	108,3	359,2	27,3	183,4	21,6	243,2	59,6	88,1
100051B	S2a. Grog in homogeneous	1294,8	5211,2	107,8	123,3	174,3	11,9	50,4	89,2	96,3	419,4	27,9	187,4	19,1	270,0	53,1	82,6
100051C	fossiliferous groundmass	1540,2	4960,2	99,6	274,1	207,4	12,1	91,1	203,8	178,7	417,1	26,5	193,4	18,0	310,6	57,2	74,9
100067		1191,6	4628,2	121,8	209,2	227,3	54,7	234,5	289,8	147,7	354,1	27,7	174,9	20,2	362,4	58,7	90,3
100042D	S2b. Grog in inhomogeneous	1449,4	5554,4	114,8	132,8	165,7	10,7	44,4	92,5	78,4	353,9	25,9	177,2	20,3	310,6	55,7	85,9
100109B	fossiliferous groundmass	1103,6	4430,2	93,0	112,9	152,2	14,6	50,8	214,3	265,6	367,1	24,2	161,6	16,9	274,2	48,4	69,8

sample	Fabric	Pr	Nd	Sm	Eu	Gd	Tb	Dy	Ho	Er	Tm	Yb	Lu	Hf	Ta	W	Th	U
100033G		9,4	40,5	8,0	1,6	6,1	0,9	5,1	1,0	2,9	0,4	2,7	0,3	4,9	1,4	2,4	12,5	2,8
100051B	S2a. Grog in homogeneous	8,9	39,7	7,9	1,5	5,9	0,9	5,1	1,1	2,7	0,5	2,9	0,4	4,9	1,4	1,9	12,9	2,5
100051C	fossiliferous groundmass	8,1	36,3	7,5	1,4	5,6	0,7	4,6	0,9	2,7	0,3	2,3	0,4	5,1	1,3	47,6	11,6	2,6
100067		9,6	42,5	9,3	1,8	5,9	0,8	5,5	1,0	2,9	0,4	3,0	0,4	5,0	1,3	2,2	14,3	3,0
100042D	S2b. Grog in inhomogeneous	8,9	39,6	6,9	1,6	5,2	0,8	5,2	1,0	2,8	0,3	2,2	0,4	4,8	1,4	1,8	12,1	2,5
100109B	fossiliferous groundmass	7,5	33,8	6,7	1,4	5,3	0,8	4,5	0,9	2,6	0,5	2,1	0,3	4,6	1,2	33,9	11,3	2,4
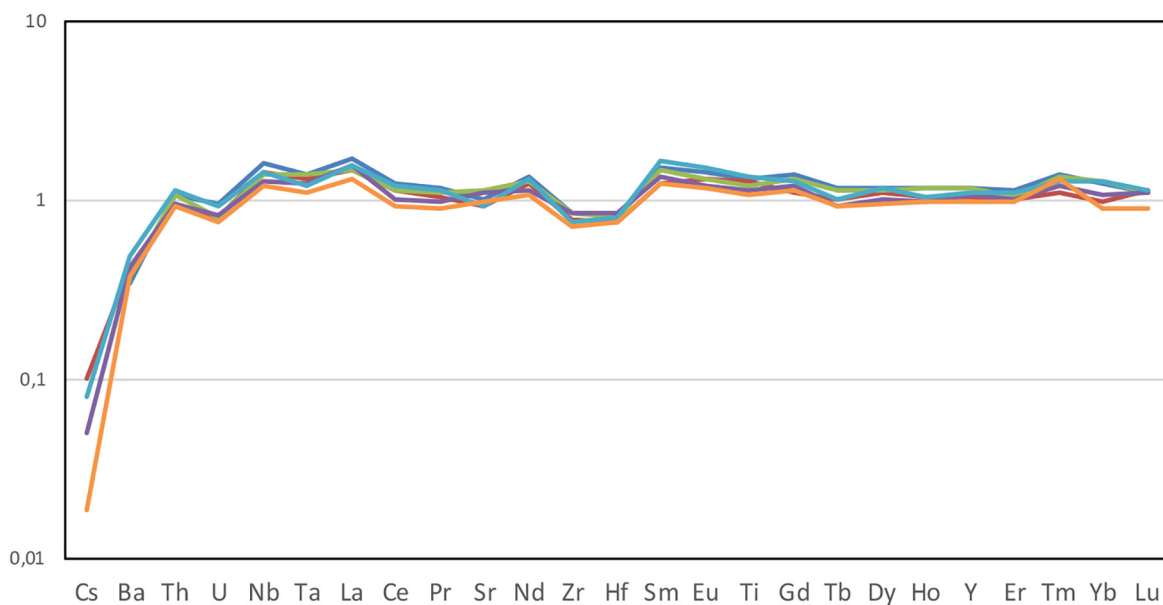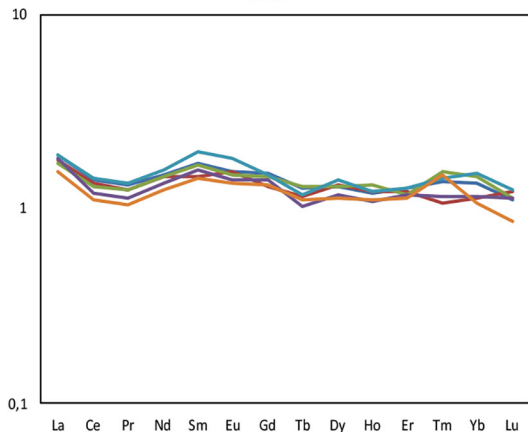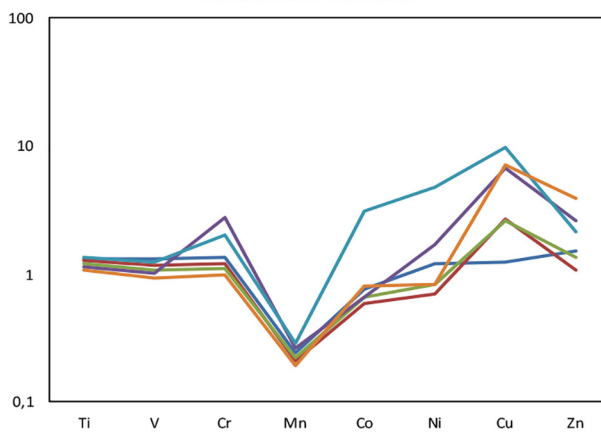
Fig. 5. Major, minor and trace elements of the six samples measured by LA-ICP-MS: composition of incompatible elements (a), composition of REE elements (b), composition of transition elements (c).
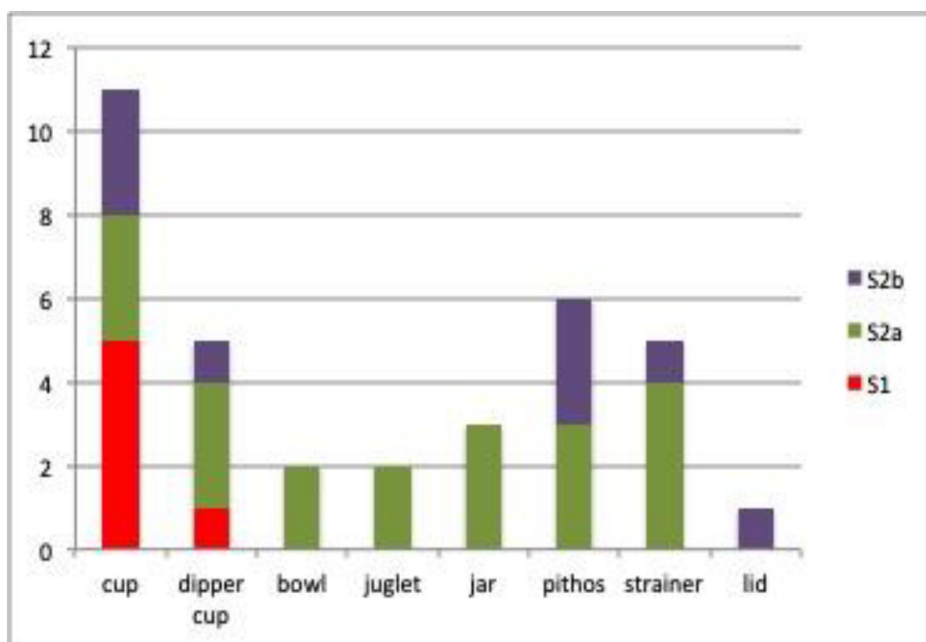
Fig. 6. Relationship between shape/function and Fabrics.

pottery has revealed a compositional assemblage with a range of different local Fabrics and only one off-island artifact. In terms of local production, the Baħrija fabrics differ from the Borġ in-Nadur ones, as the detailed compositional investigation presented here has demonstrated.

6. Conclusions

This first archaeometric study of Baħrija pottery has provided significant new data on the debate about the end of prehistory in the Maltese archipelago. This study has once again proved how tricky it can be to try classifying ceramic fabrics purely on the basis of direct examination and has also disproved some traditional assumptions.

To have proved that the examples of grey ware showing typical features of Sicilian Middle Bronze pottery production (100061B, 100050A, 100061E, 100061H), the two examples of strainer spouted jars (100051D, 100109A), and the wall fragment of painted ware (100109B) are local productions have disproved their traditional interpretation as Sicilian imports and it demonstrates that the relationship between Sicily and Malta at the end of the 2nd millennium BCE was tighter and more complicated than was previously thought (Tanasi, 2011b, 2015b). In fact, the samples in question have truly stylistic and technological features typical of the Middle and Late Bronze Age Sicilian repertoires, which means that they were either produced in Malta by Sicilian potters or crafted by Maltese potters which had direct knowledge of the Sicilian pottery. This discovery forces us to rethink the entire relationship between the two indigenous communities and to

put aside the traditional idea that Malta acted as just a passive player in the dynamics of acculturation (Evans, 1971).

With respect to the attempt to interpret the apparent break with the Borġ in-Nadur pottery production tradition that the Baħrija pottery appeared to be, analyses have demonstrated the existence of a new petrographic fabric (S1. Fossiliferous optically inactive groundmass), which was not found during other archaeometric studies on Borġ in-Nadur ceramics analysed at Borġ in-Nadur temple and in two sites in Sicily (Raneri et al., 2015). These new data reinforce the hypothesis of a break with traditional production practices, which is not just a change in shapes and style of the pottery, but is a technological change that can very likely be connected with the different potting practices of the newcomers. The absence of the other traditional fabric (grog and spathic calcite) attested at Borġ in-Nadur temple is another indicator of such technological change. However, continuation in the use of traditional fabric (S2. Grog in fossiliferous groundmass) along with the new one, testifies to a gradual amalgamation between new and old cultural habits rather than an abrupt break.

A whole new scenario has been ultimately opened by the identification of the unusual fabric with granitic rocks and quartz minerals on the pyramidal loom weight (100006A). In fact, it is now an undoubted external import which, however, cannot be traced back to Sicily, the closest geographic region with a history of close relations. Unfortunately, since it was found during the excavations carried out by Peet in 1910, the information about its context of provenance are very limited. However, it is important to highlight that all the materials retrieved during both excavations of Peet (1910) and Trump (1961)

Table 7
Comparison of the Fabrics in the present study and other sets of samples.

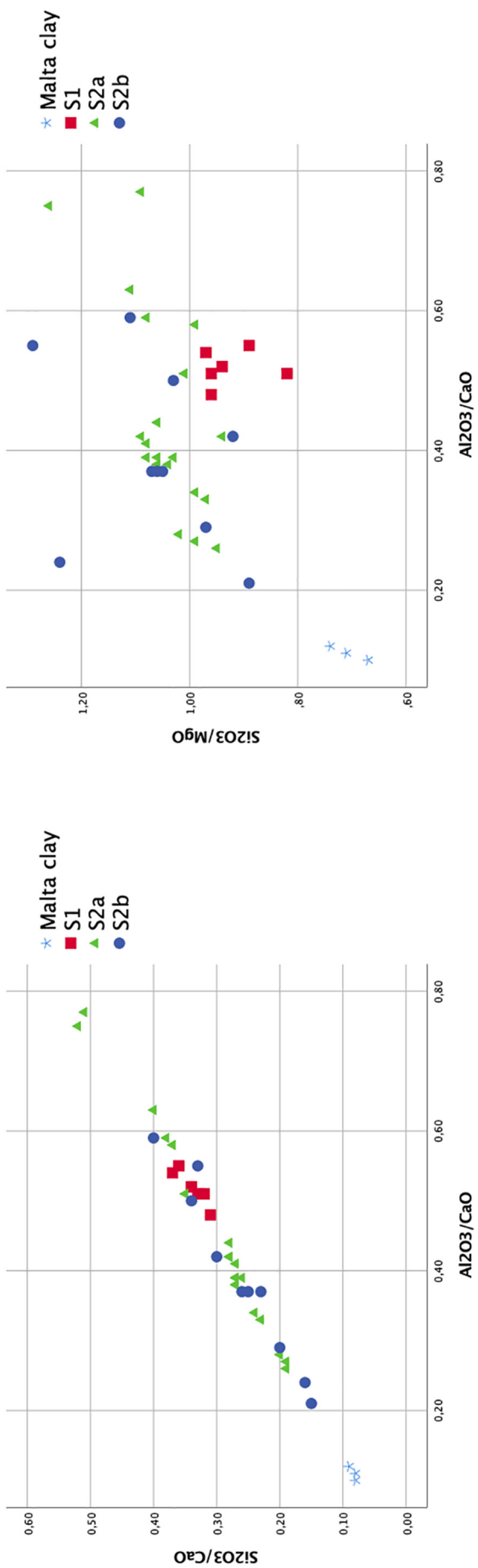|	**Baħrija** (this study)	**Borg in-Nadur** (Barone et al. 2015)	**Cannatello and Ognina Borg-in-Nadur (Malta origin)** (Barone et al. 2015)	**Cannatello Borg-in_Nadur (Malta)** (Jones et al. 2014)
S1. Fossiliferous optically inactive groundmass	X			
S2. Grog in fossiliferous groundma	X	Fabric A	Fabric A	X
S3. Grog and spatic calcite		Fabric B		

Fig. 7. Binary diagrams of the Fabrics and Malta clays (Barone et al., 2015): SiO_2/CaO vs. Al_2O_3/CaO (a), and $SiO2/MgO$ vs. Al_2O_3/CaO (b).
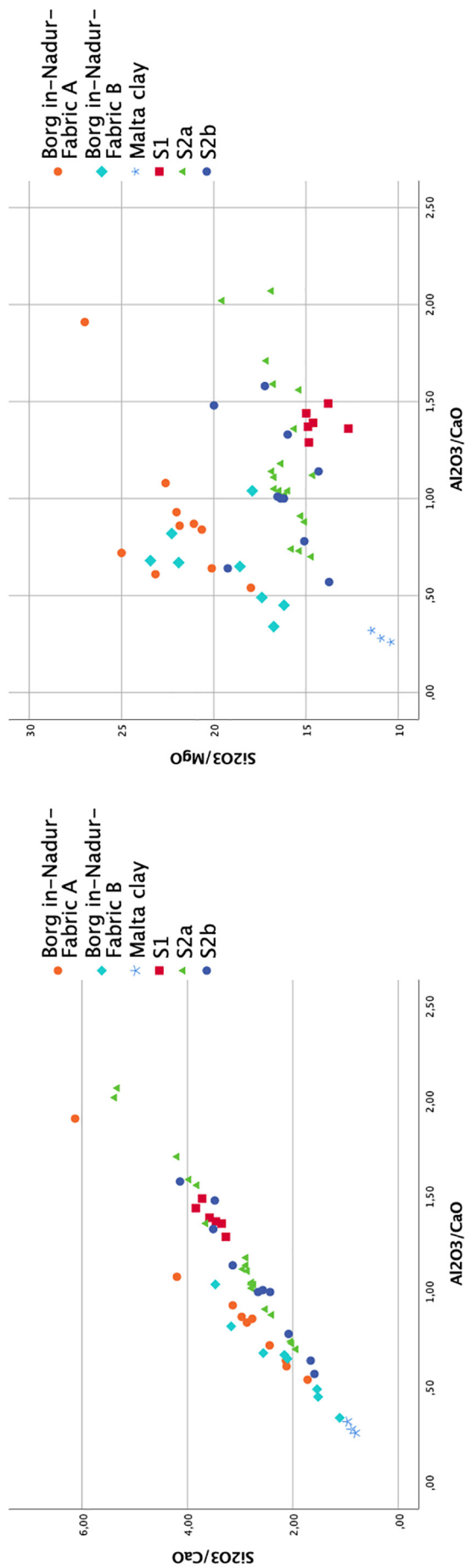

Fig. 8. Binary diagrams of this set of samples, and the dataset from Barone et al. (2015): SiO_2/CaO vs. Al_2O_3/CaO (a), and SiO_2/MgO vs. Al_2O_3/CaO (b).
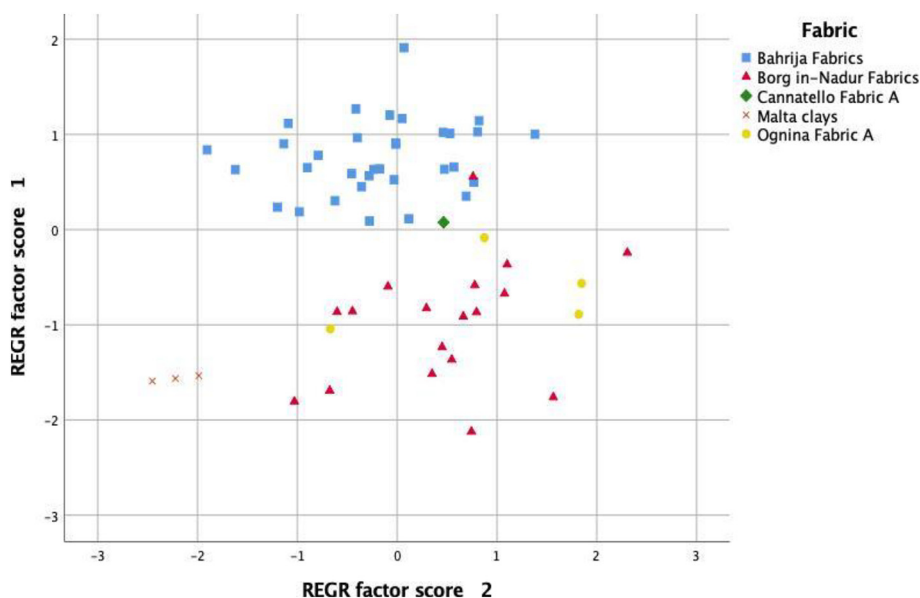
Fig. 9. Principal components analysis (PCA) based on major and minor elements of Fabrics from Baħrija, Borġ in-Nadur (Barone et al., 2015), Borġ in-Nadur type pottery from Ognina and Cannatello (Barone et al., 2015) and Malta Blue clays (Barone et al., 2015). Factor 1 (45.3%) + Zr, + Cr, -CaO, -K$_2$O. Factor 2 (17.5%) + TiO$_2$, + Si$_2$O$_3$, -CaO, −Sr.

belong to the Late Borġ in-Nadur/Baħrija period, without any findings attributable to earlier or later phases. At this stage and with the limited comparative data available, it just possible to suggest that it could have been introduced in Malta from other areas with which the island was in contact in that period, such as the North African coast. Future research and more in-depth analyses of the Baħrija, currently ongoing, will certainly shed more light on such a potentially very high impact discovery.

References

Barone, G., Mazzoleni, P., Raneri, S., Tanasi, D., Giuffrida, A., 2015. Archaeometric characterization of Middle Bronze Age pottery from the settlement at Borġ in-Nadur. In: Tanasi, D., Vella, N.C. (Eds.), The Late Prehistory of Malta: Essays on Borġ in-Nadur and Other Sites. Archaeopress, Oxford, pp. 99–112.

Bonanno, A., 2008. Insularity and isolation: Malta and Sicily in prehistory. In: Militello, P., Bonanno, A. (Eds.), Malta negli Iblei. Gli Iblei a Malta. Officina di Studi Medievali, Palermo, pp. 27–37.

Bonanno, A., 2017. From prehistoric to historic Malta: a discussion of the sources. In: Mizzi, D., Vella, N.C., Zammit, M.R., Frendo, A.J. (Eds.), "What Mean these Stones?" (Joshua 4:6, 21): Essays on Texts, Philology, and Archaeology in Honour of Anthony J. Frendo. Peeters, Leuven, pp. 243–254.

Brunelli, D., Levi, S.T., Fragnoli, P., Renzulli, A., Santi, P., Paganelli, E., Martinelli, M.C., 2013. Bronze Age pottery from the Aeolian Islands: definition of Temper Compositional Reference Units by an integrated mineralogical and microchemical approach. Appl. Phys. 113, 855–863.

Bruno, B., Capelli, C., 2000. Nuovi tipi di anfore a Malta. In: D'Amico, C. Tampellini (Ed.),

6a Giornata Le Scienze della terra e l'archeometria Este 1999, Este, pp. 59–65.

Buhagiar, K., 2012. Caves in context: the Late Medieval Maltese scenario. In: Bergsvik, K.A., Skeates, R. (Eds.), Caves in Context, Cultural Significance of Caves and Rockshelters in Europe. Oxbow Books, pp. 153–165.

Chunshu, W., Mingcai, Y., Wenhua, Z., Qinghua, C., Tiexin, G., 1996. Chinese synthetic silicate and limestone certified reference materials for spectral analysis. Geostand. Newslett. 20, 57–64.

Condie, K.C., 2015. Plate Tectonics and Crustal Evolution. Elsevier, Amsterdam, pp. 16–17.

Evans, J.D., 1953. The prehistoric culture-sequence in the Maltese Archipelago. Proceedings of the Prehistoric Society 19, 41–94.

Evans, J.D., 1971. The Prehistoric Antiquities of the Maltese Islands. A Survey. The Athlone Press, London.

Gazzulla Barreda, M.F., Rodrigo Edo, M., Orduña Cordero, M., Ventura Vaquer, M.J., 2016. Determination of minor and trace elements in geological materials used as raw ceramic materials. Boletín de la Sociedad Española de cerámica y vidrio 55, 185–196.

Hunt, A.M.W., 2017. The Oxford Handbook of Archaeological Ceramic Analysis. Oxford University press, pp. 48–57.

Jones, R., Levi, S.T., Bettelli, M., Vagnetti, L., 2014. Italo–Mycenaean Pottery, the Archaeological and Archaeometric Dimensions. Incunabula Graeca CIII, CNR–Istituto di Studi sul Mediterraneo Antico, Rome, pp. 229–233.

Levi, S.T., Fragnoli, P., 2010. Le analisi archeometriche delle ceramiche. In: Martinellli, M.C. (Ed.), Archeologia dellle Isole Eolie. Il villaggio dell'età del Bronzo Medio di Portella a Salina. Ricerche 2006 e 2008. Rebus Muggio (MB), pp. 219–232.

Levi, S.T., Jones, R.E., 2005. Analisi archeometrica delle ceramiche. In: Martinelli, M.C. (Ed.), Il villaggio dell'età del Bronzo medio di Portella a Salina nelle Isole Eolie. Origines, Firenze, pp. 241–262.

Levi, S.T., Bettelli, M., Cannavò, V., Di Renzoni, A., Ferranti, F., Martinelli, M.C., Ollà, A., Tigano, D., 2017. Stromboli: gateway for the Mycenaean early connections through the Messina's Strait. In: Fotidias, M., Laffineur, R., Lolos, Y., Vlachopoulos, A. (Eds.), HESPEROS. The Aegean Seen from the West. 16th International Aegean Conference. Aegaeum, Annales liégeoises d'archéologie égéenne, Ionnina, pp. 147–154.

Levi, S.T., Cannavò, V., Brunelli, D., 2019. Atlas of Ceramic Fabrics 2. Italy: Southern Tyrrhenian-Neolithic-Bronze Age. Archaeopress, Oxford.

Malone, C., Stoddart, S., Bonanno, A., Gouder, T., Grima, R., Trump, D., 2009. Introduction: the intellectual and historical context. In: Malone, C., Stoddart, S., Bonanno, A., Trump, D., Gouder, T., Pace, A. (Eds.), Mortuary Customs in Prehistoric Malta: Excavations at the Brochtorff Circle at Xaghra (1987–94). McDonald Institute for Archaeological Research, Cambridge, pp. 1–16.

Malta. Oil Exploration Directorate, 1993. Geological Map of the Maltese Islands: 1:25,000. Malta: Oil Exploration Directorate, Valletta.

Papadopoulou, D.N., Zachariadis, G.A., Anthemidis, A.N., Tsirliganis, N.C., Stratis, J.A., 2004. Microwave-assisted versus conventional decomposition procedures applied to a ceramic potsherd standard reference material by inductively coupled plasma atomic emission spectrometry. Anal. Chim. Acta 505, 173–181.

Pedley, M., Clarke, M.H., Galea, P., 2002. Limestone Isles in a Crystal Sea. P.E.G., Malta.

Peet, T.E., 1910. Contributions to the study of the prehistoric period in Malta. In: Papers of the British School at Rome V, pp. 141–163.

Pirone, F., Tykot, R.H., 2017. Trace elemental characterization of Maltese pottery from the Late Neolithic to Middle Bronze Age. Open Archaeology 3, 202–221.

Quinn, P.S., 2013. Ceramic Petrography: The Interpretation of Archaeological Pottery & Related Artefacts in Thin Section. Archaeopress, Oxford.

Raneri, S., Barone, G., Mazzoleni, P., Tanasi, D., Costa, E., 2015. Mobility of men versus mobility of goods: archaeometric characterization of Middle Bronze Age pottery in Malta and Sicily (15th–13th century BC). Periodico di Mineralogia 84 (1), 23–44 2015.

Recchia, G., Fiorentino, G., 2015. Archipelagos adjacent to Sicily around 2200 BC: attractive environments or suitable geo-economic locations? In: Meller, H.H., Arz, H.W., Jung, R., Risch, R. (Eds.), 2200 BC. A Climatic Breakdown as a Cause for the Collapse of the Old Works? Tagungen des Landesmuseums für Vorgeschichte Halle Band 12/I, pp. 305–319.

Rudnick, R.L., Gao, S., 2003. Composition of the continental crust. In: Heinrich Holland, D., Turekian, K.K. (Eds.), Treatise on Geochemistry 3. Elsevier, Amsterdam, pp. 1–64.

Sagona, C., 2008. Malta: Between and rock and a hard place. In: Sagona, C. (Ed.), Beyond the Homeland: Markers in Phoenician Chronology. Ancient Near Eastern Studies Supplement, vol. 28. Peeters, Louvain, pp. 487–536.

Sagona, C., 2011. Observations on the Late Bronze Age and Phoenician-Punic pottery in Malta. In: Sagona, C. (Ed.), Ceramics of the Phoenician-Punic World: Collected Essays. Ancient near Eastern Studies Supplement, vol. 36. Peeters, Louvain, pp. 397–432.

Sagona, C., 2015. The Archaeology of Malta from Neolithic Through the Roman Period. Cambridge University Press, New York.

Tanasi, D., 2011a. The prehistoric pottery. In: Tanasi, D., Vella, N.C. (Eds.), Site, Artefacts, Landscape: Prehistoric Borġ in- Nadur, Malta, Praehistorica Mediterranea 3. Polimetrica Monza, pp. 71–158.

Tanasi, D., 2011b. Living and dying in a foreign country. Maltese immigrants in Middle Bronze Age Sicily. In: Tanasi, D., Vella, N.C. (Eds.), Site, Artefacts, Landscape: Prehistoric Borġ in-Nadur, Malta. Polimetrica, Monza, pp. 283–337 2011.

Tanasi, D., 2015a. The pottery from the excavation campaign of David H. Trump (1959) at the settlement of Borġ in-Nadur. In: Tanasi, D., Vella, N.C. (Eds.), The Late Prehistory of Malta: Essays on Borġ in-Nadur and Other Sites. Archaeopress, Oxford, pp. 35–98 2015.

Tanasi, D., 2015b. Borġ in-Nadur pottery abroad: A report from the Sicilian necropoleis of Thapsos and Matrensa. In: Tanasi, D., Vella, N.C. (Eds.), The Late Prehistory of Malta: Essays on Borġ in-Nadur and Other Sites. Archaeopress, Oxford, pp. 173–784 2015.

Tanasi, D., 2018. Taking Maltese prehistory out of the box. Towards a definition of Borġ in-Nadurarchaeological facies. In: Vella, N.C., Frendo, A.J., Vella, H.C.R. (Eds.), Lure of the Antique: Essays on Malta and the Mediterranean in Honour of Anthony Bonanno. Peeters Publishers, Leuven, pp. 183–197.

Tanasi, D., 2019. Pottery from the T.E. Peet and D.H. Trump excavations at Baħrija. In: Tanasi, D., Cardona, D. (Eds.), The Maltese Archipelago at the Dawn of History. Excavations at Bahrija (1909 and 1959). Archaeopress, Oxford (in press).

Tanasi D., Vella N.C. 2014. Islands and mobility: exploring bronze age connectivity in the south-Central Mediterranean, in Van Dommelen P., Knapp B. (eds.), The Cambridge Prehistory of the Bronze and Iron Age Mediterranean. Cambridge: Cambridge University Press, pp. 53–73.

Trump, D.H., 1961. The later prehistory of Malta. Proceedings of the Prehistoric Society 27, 253–262.

Tusa, S., 1992. Le fasi formative della cultura elima alla luce di recenti rinvenimenti. In: AA.VV., Giornate Internazionali di Studi sull'Area Elima, Gibellina 19–22 Settembre 1991, Pisa-Gibellina 1992, pp. 603–615.

Vella, N.C., 2005. Phoenician and Punic Malta. Journal of Roman Archaeology 18, 436–450.

Vella, N.C., Tanasi, D., Anastasi, M., 2011. Mobility and transitions: the south central Mediterranean on the eve of history. In: Tanasi, D., Vella, N.C. (Eds.), Site, Artefacts, Landscape: Prehistoric Borġ in-Nadur, Malta. Polimetrica, Monza, pp. 251–282 2011.

Whitbread, I.K., 1989. A proposal for the systematic description of thin sections towards the study of ancient ceramic technology. In: Maniatis, Y. (Ed.), Archaeometry: Proceedings of the 25th International Symposium. Elsevier, Amsterdam, pp. 127–138.

Williams, J.L., 1980. A petrological examination of the prehistoric pottery from the excavations in the Castello and Diana Plain of Lipari - an interim report. In: Bernabò Brea, L., Cavalier, M. (Eds.), Meligunìs Lipára IV, Palermo, pp. 847–868.

Williams, J.L., 1991. The petrographic analysis of Capo Graziano Pottery from Filicudi and Milazzese Pottery from Panarea. In: Bernabò Brea, L., Cavalier, M. (Eds.), Meligunìs Lipára VI, Palermo, pp. 239–259.